Non-Convex Plasticity and Dislocation Structures

M. Ortiz

California Institute of Technology

2002 GAMM Annual Meeting

University of Augsburg

Stuttgart, Germany

March 25-26, 2002

Outline

- *Microstructure:* The breakdown of Drucker's postulates of classical plasticity.
- *Non-convex plasticity*: Beyond Drucker.
- *Non-local regularization*: Scaling and size effect.
- *Validation*: Predictions of the theory:
  - Dipolar dislocation walls in fatigued single crystals
  - Cold-rolled polycrystals:
    - Misorientation angle distributions, evolution
    - Lamellar size distributions, evolution
- *Direct numerical simulation* of microstructure: Subgrid implementation.

Subgrain dislocation structures - Fatigue

Dipolar dislocation walls

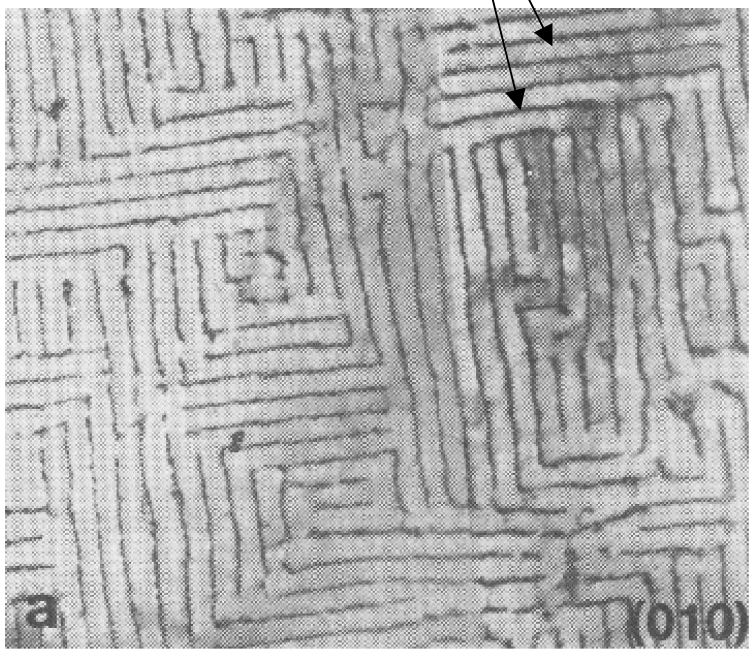

Labyrinth structure in fatigued copper single crystal (Jin and Winter, 1984)

Nested bands in copper single crystal fatigued to saturation (Ramussen and Pedersen, 1980)

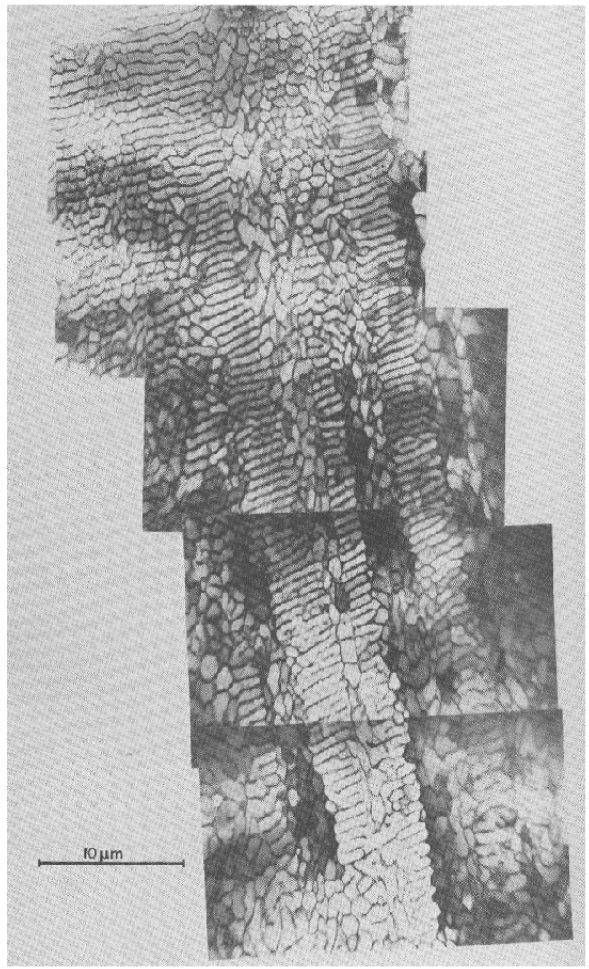

Subgrain dislocation structures - Static

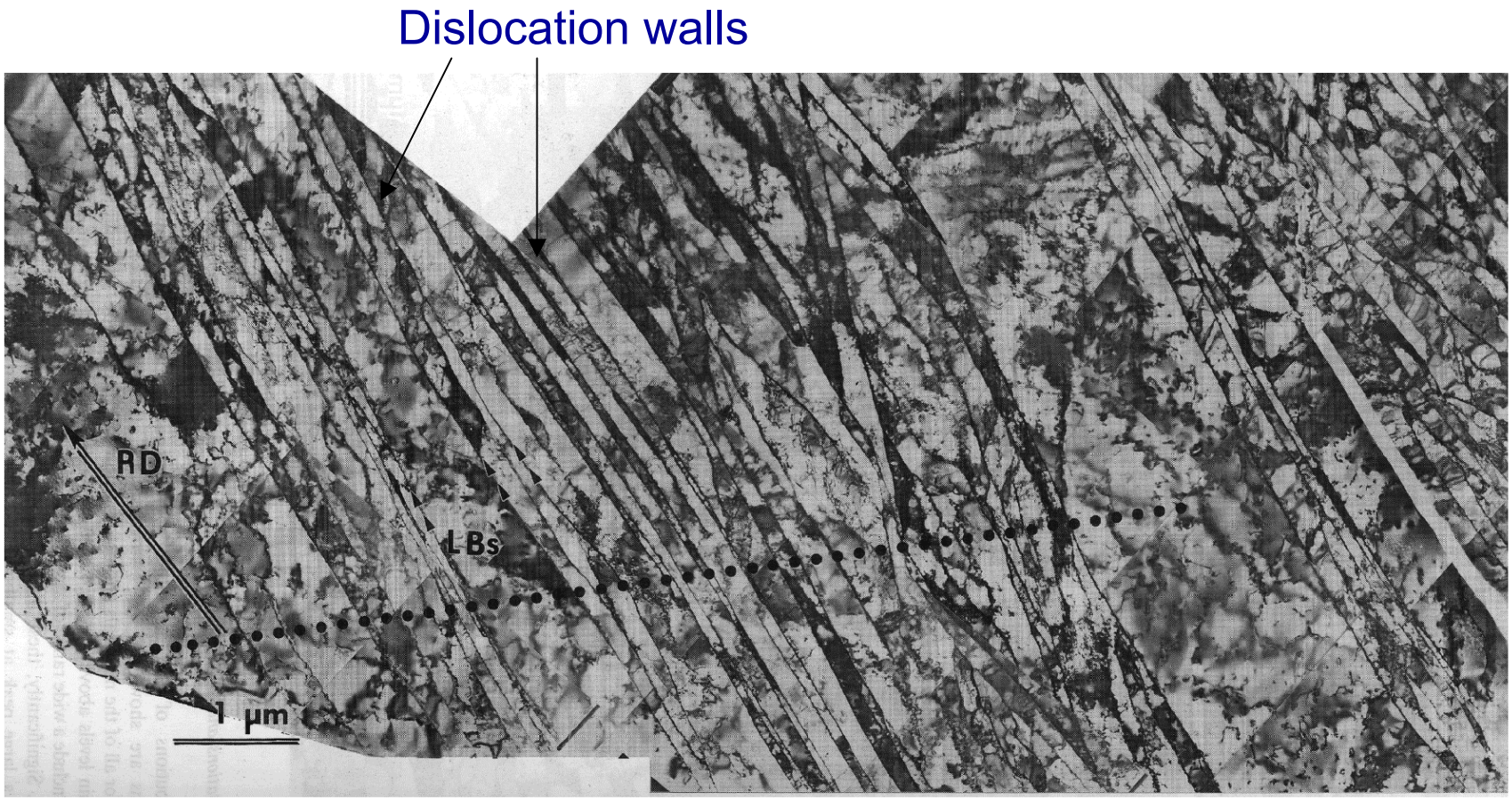

90% cold rolled Ta (Hughes and Hansen, 1997)

Subgrain dislocation structures - Shock

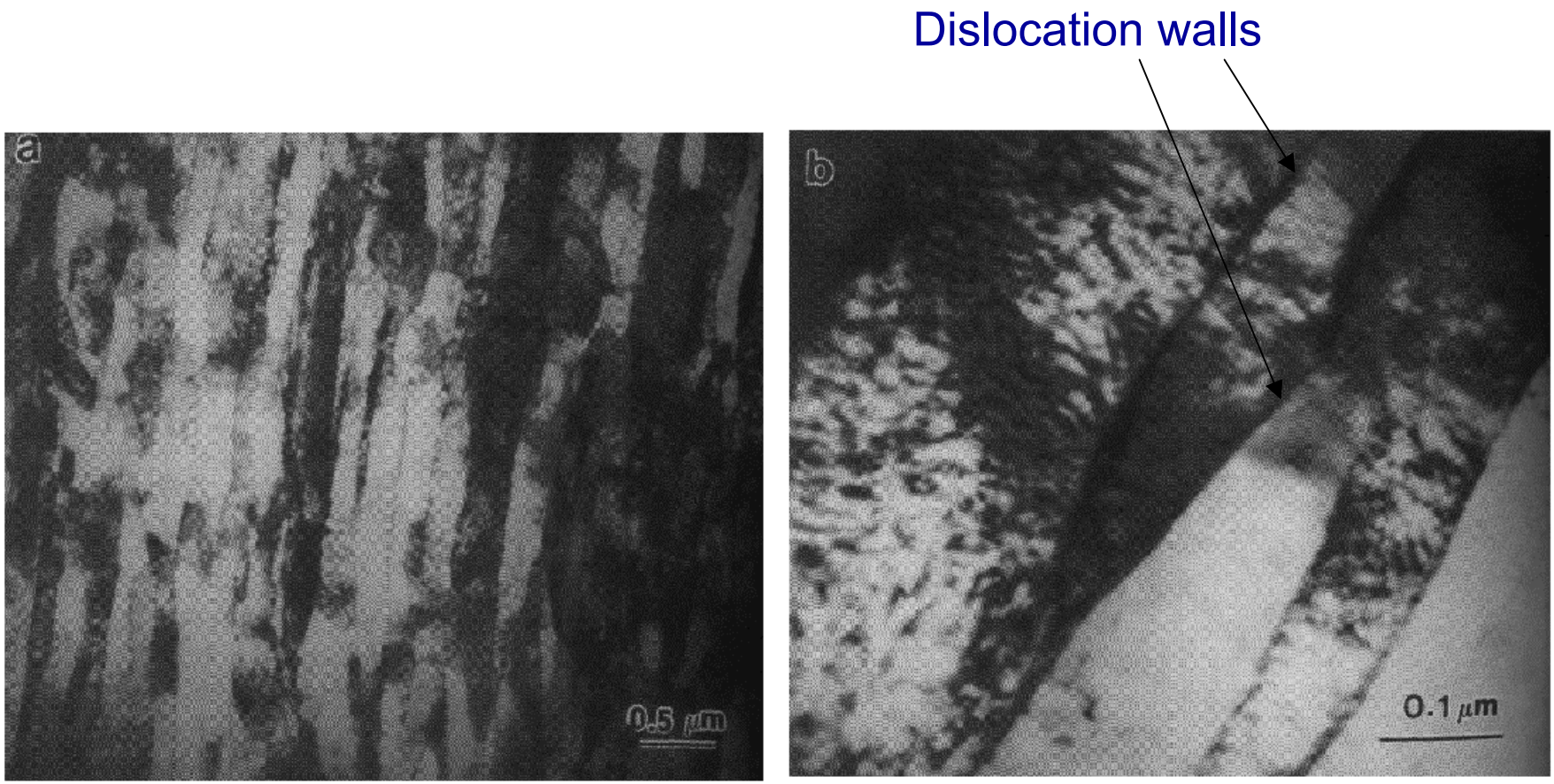

Shocked Ta (Meyers et al., 1995)

Subgrain dislocation structures

- Dislocation structures are universally observed in single crystals under a variety of conditions, including:
  - *Fatigue in specimens oriented for multiple slip*
  - *Large monotonic deformations*
  - *Shock loading*
- Objective: To develop a theory which
  - *Accounts for dislocation structures*
  - *Predicts macroscopic effective behavior, including:*
    - *Scaling (e.g., Taylor hardening)*
    - *Size effects (e.g., Hall-Petch scaling)*
  - *Can be integrated into large-scale numerical simulations*
- Basic strategy: Formulate problem in *variational form*, use tools from *modern calculus of variations.*

Viscoplasticity – Initial BVP

- Body $\Omega \subset \mathbb{R}^3$, mapping $\boldsymbol{y} : \Omega \times [t_0, t_f] \to \mathbb{R}^3$.
- $A(\boldsymbol{F}, \boldsymbol{F}^p, \boldsymbol{\gamma}) \equiv$ Free-energy density.
- Flow rule: $\dot{\boldsymbol{F}}^p \boldsymbol{F}^{p-1} = \sum_\alpha \dot{\gamma}^\alpha \boldsymbol{s}^\alpha \otimes \boldsymbol{m}^\alpha$.
- Conjugacy: $\delta A = \boldsymbol{P} \cdot \delta \boldsymbol{F} - \boldsymbol{Y} \cdot \delta \boldsymbol{\gamma}$.
- $\psi(\boldsymbol{Y}) \equiv$ Kinetic potential.
- Initial Boundary-Value problem: For $t \geq 0$,

$$\inf_{\boldsymbol{y} \in X} \int_\Omega A(D\boldsymbol{y}, \boldsymbol{F}^p, \boldsymbol{\gamma}) + \text{forcing terms}$$

$$\dot{\boldsymbol{\gamma}} = \partial\psi\Big(\boldsymbol{Y}(D\boldsymbol{y}, \boldsymbol{F}^p, \boldsymbol{\gamma})\Big), \quad \forall \boldsymbol{x} \in \Omega$$

Variational Constitutive Updates

- Discretize time: $t_0, \ldots, t_n, t_{n+1} = t_n + \triangle t, \ldots$
- Incremental work-of-deformation density:

$$W_n(\boldsymbol{F}_{n+1}) = \inf_{paths} \int_{t_n}^{t_{n+1}} \boldsymbol{P} \cdot \dot{\boldsymbol{F}}\, dt$$

- Alternatively: $\boldsymbol{F}^p_{n+1} = \exp\left\{\sum_\alpha \triangle\gamma^\alpha \boldsymbol{s}^\alpha \otimes \boldsymbol{m}^\alpha\right\} \boldsymbol{F}^p_n$

$$W_n(\boldsymbol{F}_{n+1}) = \inf_{\boldsymbol{\gamma}_{n+1} \geq \boldsymbol{\gamma}_n} \left\{ A_{n+1} - A_n + \triangle t\, \psi^*\left(\frac{\triangle \boldsymbol{\gamma}}{\triangle t}\right)\right\}$$

- Fundamental property:

$$\boldsymbol{P}_{n+1} = \frac{\partial W_n}{\partial \boldsymbol{F}_{n+1}}(\boldsymbol{F}_{n+1})$$

Incremental Variational Problem

- Incremental work functional:

$$I_n[\boldsymbol{y}_{n+1}] = \int_\Omega W_n(D\boldsymbol{y}_{n+1})\, dx + \text{forcing terms}$$

- Incremental variational problem:

$$\boxed{\inf_{\boldsymbol{y}_{n+1}\in X} I_n[\boldsymbol{y}_{n+1}]}$$

- Euler-Lagrange equations:

$$\delta I_n = \int_\Omega \boldsymbol{P}_{n+1} \cdot D\delta\boldsymbol{y}_{n+1}\, dx + \text{forcing terms} = 0$$

$\Rightarrow$ weak form of equilibrium equations.

Classical plasticity

- Linearized kinematics, $\boldsymbol{\epsilon} = \boldsymbol{\epsilon}^e + \boldsymbol{\epsilon}^p$,

$$\boldsymbol{\epsilon}^p_{n+1} = \boldsymbol{\epsilon}^p_n + \sum_\alpha \triangle\gamma^\alpha \text{sym}(\boldsymbol{s}^\alpha \otimes \boldsymbol{m}^\alpha)$$

- Incremental work-of-deformation density: $W_n(\boldsymbol{\epsilon}_{n+1}) =$

$$\inf_{\boldsymbol{\gamma}_{n+1} \geq \boldsymbol{\gamma}_n} \left\{ W^e(\boldsymbol{\epsilon}^e_{n+1}) + \underbrace{W^p(\boldsymbol{\gamma}_{n+1})}_{} + \underbrace{\triangle t\, \psi^* \left(\frac{\triangle \boldsymbol{\gamma}}{\triangle t} \right)}_{} \right\}$$

- Drucker's second postulate: Convex!
- Drucker's first postulate: Convex!
- Convexity $\Rightarrow$ inf $I_n[\boldsymbol{u}_{n+1}]$ is attained, minimizer is unique $\Rightarrow$ NO MICROSTRUCTURE!

Strong latent hardening

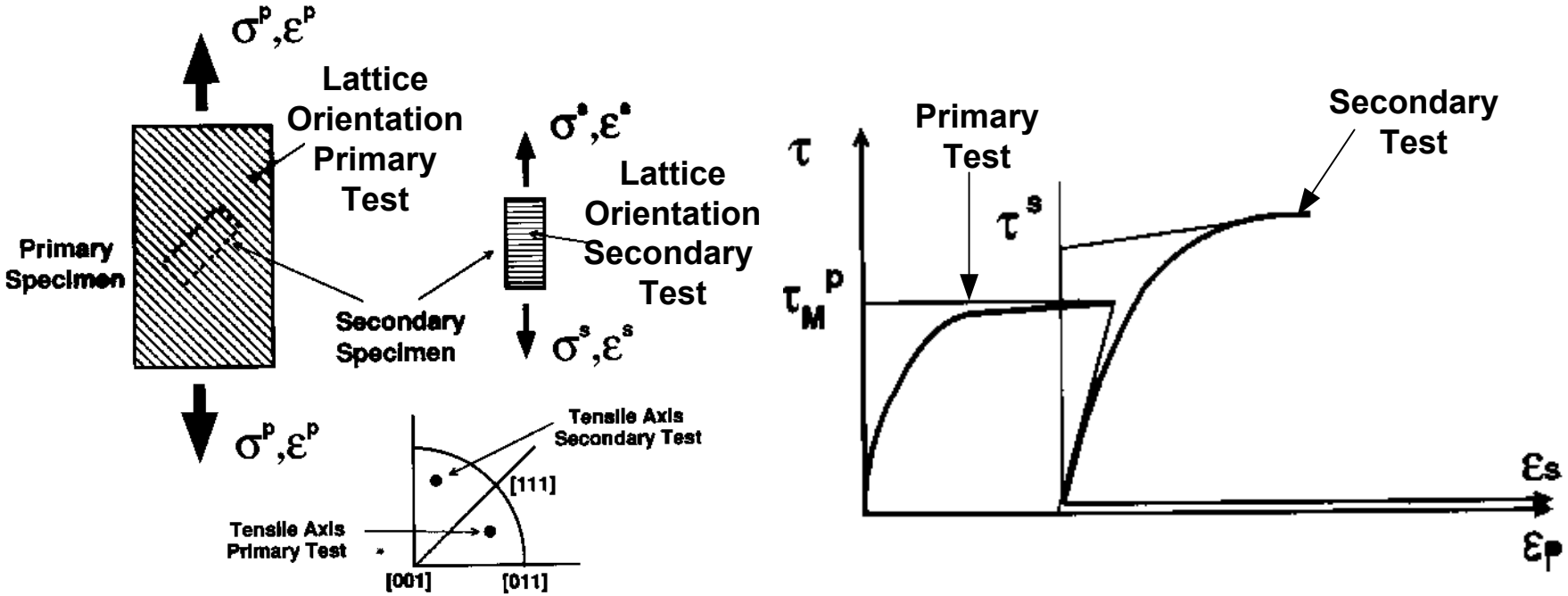

Kocks, U. F., "Polyslip in single crystals", *Acta Metallurgica*, **8** (1960) 345.

Kocks, U. F., "Latent hardening and secondary slip in aluminum and silver" *Trans. Metall. Soc. AIME*, **230** (1964) 1160.

Franciosi, P. Berveiller, M., Zaoui, A., "Latent hardening in copper and aluminum single crystals", *Acta Metallurgica*, **28** (1980) 273.

Non-convex plasticity

- Incremental work-of-deformation density: $W_n(\boldsymbol{F}_{n+1}) =$

$$\inf_{\gamma_{n+1}\geq\gamma_n}\left\{\underbrace{W^e(\boldsymbol{F}^e_{n+1})}_{\text{QUASI-CONVEX}}+\underbrace{W^p(\gamma_{n+1})}_{\text{NON-CONVEX!}}+\underbrace{\triangle t\,\psi^*\left(\frac{\triangle\gamma}{\triangle t}\right)}_{\text{CONVEX}}\right\}$$

- Strong latent hardening: $\dfrac{\partial^2 W^p}{\partial\gamma^\alpha\partial\gamma^\beta} > \dfrac{\partial^2 W^p}{\partial\gamma^\alpha\partial\gamma^\alpha}, \quad \alpha\neq\beta$

- Non-quasiconvexity of $W_n(\boldsymbol{F}_{n+1}) \Rightarrow I_n[\boldsymbol{y}_{n+1}]$ lacks (weak) lower semi-continuity $\Rightarrow \inf I_n[\boldsymbol{y}_{n+1}]$ is not attained $\Rightarrow$ MICROSTRUCTURE!

Incremental energy landscape

- Example: FCC crystal deforming on $(1\bar{1}0)$-plane

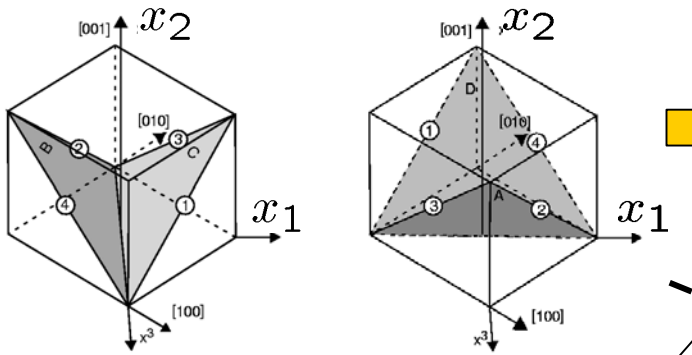

$$\boldsymbol{F}^p = \boldsymbol{I} + \gamma^\alpha \boldsymbol{s}^\alpha \otimes \boldsymbol{m}^\alpha$$

(Single slip)

PREFERRED DEFORMATIONS!

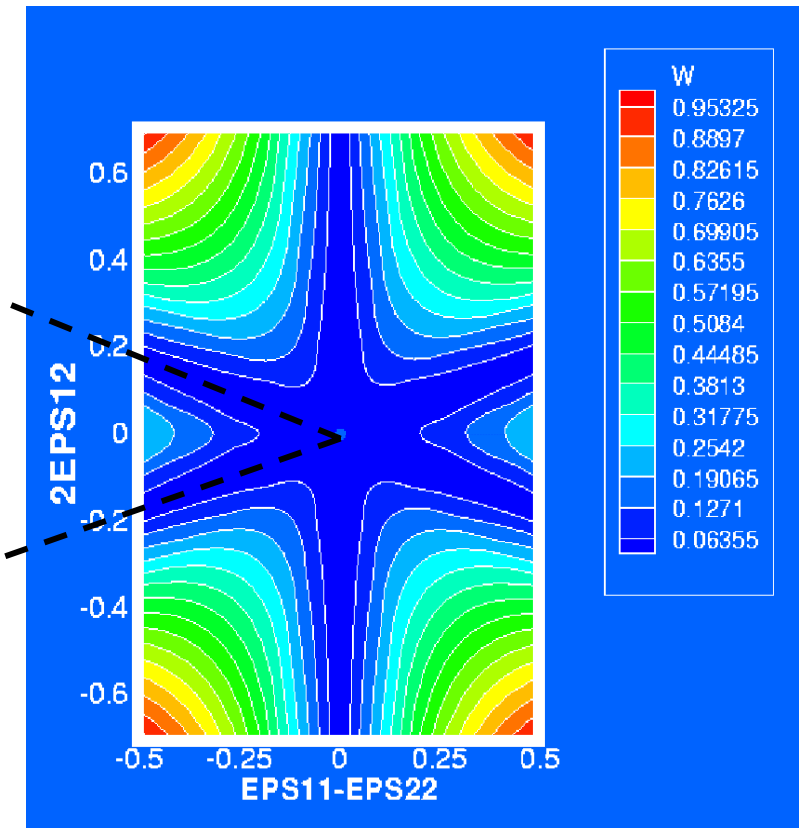

Michael Ortiz
GAMM 2002

Patchy slip

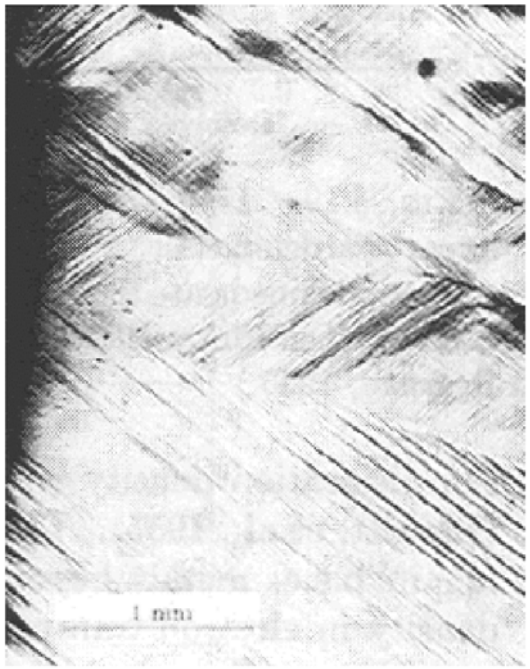

(Saimoto, 1963)

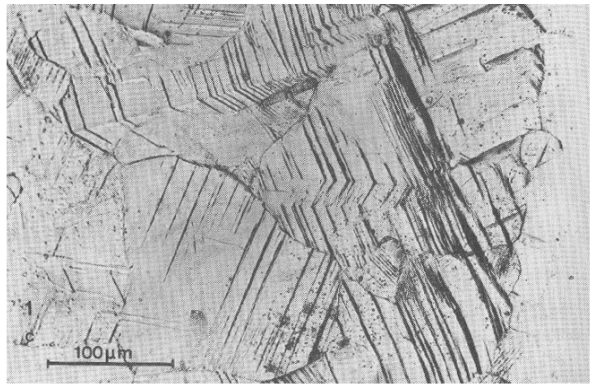

(Ramussen and Pedersen, 1980)

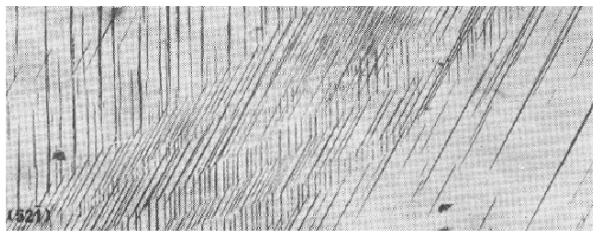

(Jin and Winter, 1984)

- **Latent hardening**: *"These results prove the reality of latent-hardening, in the sense that the slip lines of one system experience difficulty in breaking through the active slip lines of the other one"* (Piercy, G. R., Cahn, R. W., and Cottrell, A. H., *Acta Metallurgica*, **3** (1955) 331-338).

The constrained/regularized theory

- *Infinite* latent hardening $\Rightarrow$ local single slip.
- Flow rule: $\boldsymbol{F}^p_{n+1} = (\boldsymbol{I} + \triangle\gamma^\alpha \boldsymbol{s}^\alpha \otimes \boldsymbol{m}^\alpha)\boldsymbol{F}^p_n$
- Incremental work-of-deformation density: $W_n(\boldsymbol{F}_{n+1}) =$

$$\inf_{\substack{\gamma^\alpha_{n+1} \geq \gamma^\alpha_n \\ (\boldsymbol{s}^\alpha, \boldsymbol{m}^\alpha)}} \left\{ W^e(\boldsymbol{F}^e_{n+1}) + W^p(\boldsymbol{\gamma}_{n+1}) + \triangle t\, \psi^* \left(\frac{\triangle \boldsymbol{\gamma}}{\triangle t} \right) \right\}$$

- Incremental problem: $\inf_{\boldsymbol{y}_{n+1} \in W^{1,\infty}(\Omega)} I_n[\boldsymbol{y}_{n+1}]$, where

$$I_n[\boldsymbol{y}_{n+1}] = \int_\Omega \left\{ W_n(D\boldsymbol{y}_{n+1}) + \frac{T}{b} |\mathrm{curl} \boldsymbol{F}^p_{n+1}| \right\} dx$$

DISLOCATION WALL ENERGY

Relaxed incremental problem

- Relaxed problem: $\inf_{\boldsymbol{y}_{n+1}\in W^{1,\infty}(\Omega)} \int_\Omega QW_n(D\boldsymbol{y}_{n+1})\,dx$

  where

$$QW_n(\boldsymbol{F}_{n+1}) = \frac{1}{|E|} \inf_{\boldsymbol{u}\in W_0^{1,\infty}(E)} I_n[\boldsymbol{F}_{n+1}\boldsymbol{x} + \boldsymbol{u}]$$

- Relaxed energy density: Minimum energy density attainable by considering all microstructures

- No constructive method is known for relaxing general energy densities $\Rightarrow$ Special microstructures.

Sequential laminates

- Special microstructures: *Sequential laminates*.

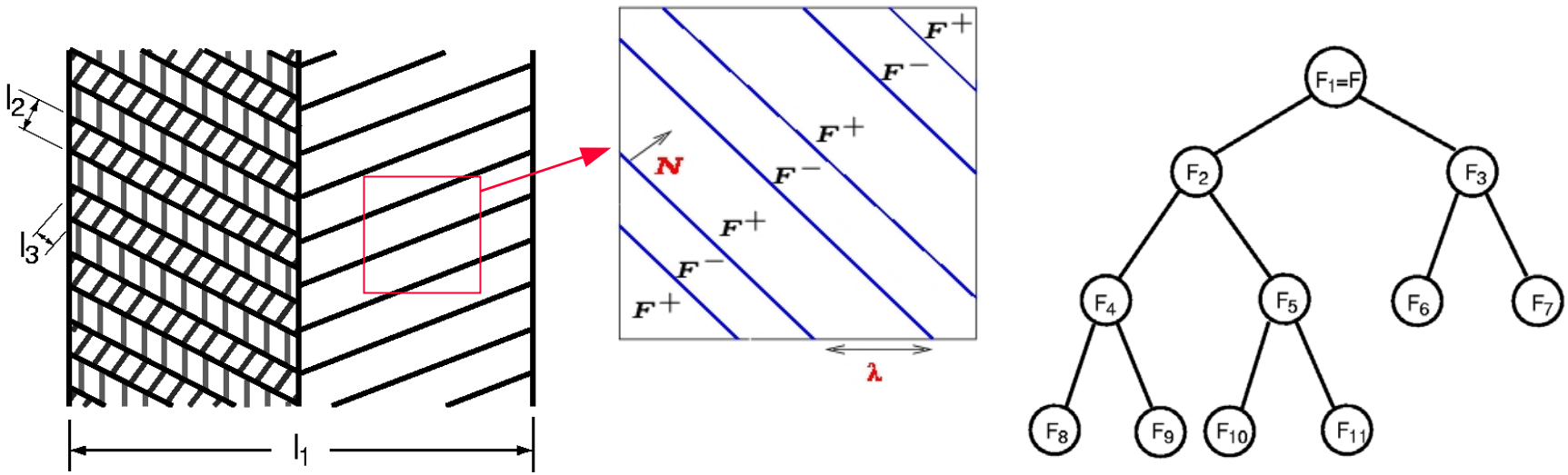

Sequential laminate ⟷ Graph G of laminate

- Compatibility: $\boldsymbol{F}_i^+ - \boldsymbol{F}_i^- = \boldsymbol{a}_i \otimes \boldsymbol{N}_i$
- Averaging: $\boldsymbol{F}_i = \lambda_i^- \boldsymbol{F}_i^- + \lambda_i^+ \boldsymbol{F}_i^+$

$$1 = \lambda_i^- + \lambda_i^+$$

Laminates - Numerical implementation

- Laminate energy *at fixed* G:

$$GW_n(\boldsymbol{F}_{n+1}) = \sum_{\text{leaves}} \nu_l W_n(\boldsymbol{F}_l)$$

  where $\nu_l \equiv$ volume-fraction of leaf l.

- Laminate equilibrium *at fixed* G: $\quad \delta GW_n = 0 \Rightarrow$

  - Tractions: $[\![\boldsymbol{P}_i]\!] \cdot \boldsymbol{N}_i = \boldsymbol{0}$

  - Configurational forces: $[\![W_i]\!] - \langle \boldsymbol{P}_i \rangle \cdot [\![\boldsymbol{F}_i]\!] = 0$

  - Configurational torques: $\boldsymbol{a}_i \cdot [\![\boldsymbol{P}_i]\!] \times \boldsymbol{N}_i = \boldsymbol{0}$

Laminates – Numerical implementation

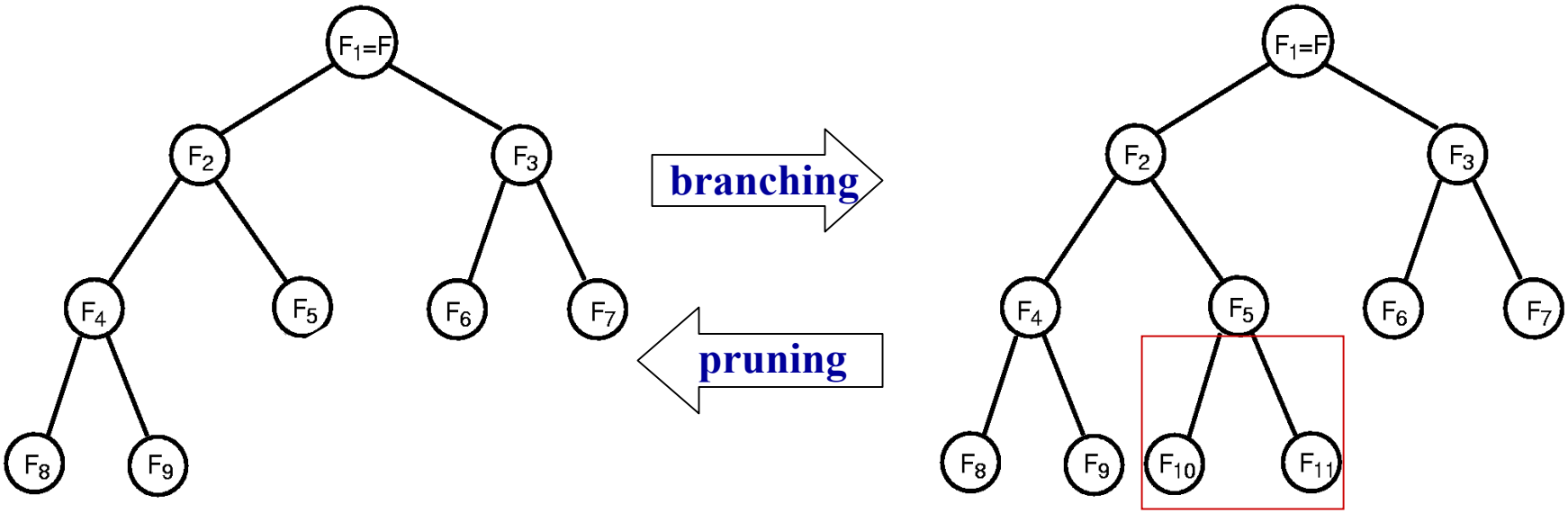

- Rules for *evolving* the laminate graphs G:
  - Accept branching iff it lowers laminate energy.
  - Prune a subtree if its volume fraction goes to 0.

Microstructure-size calculation

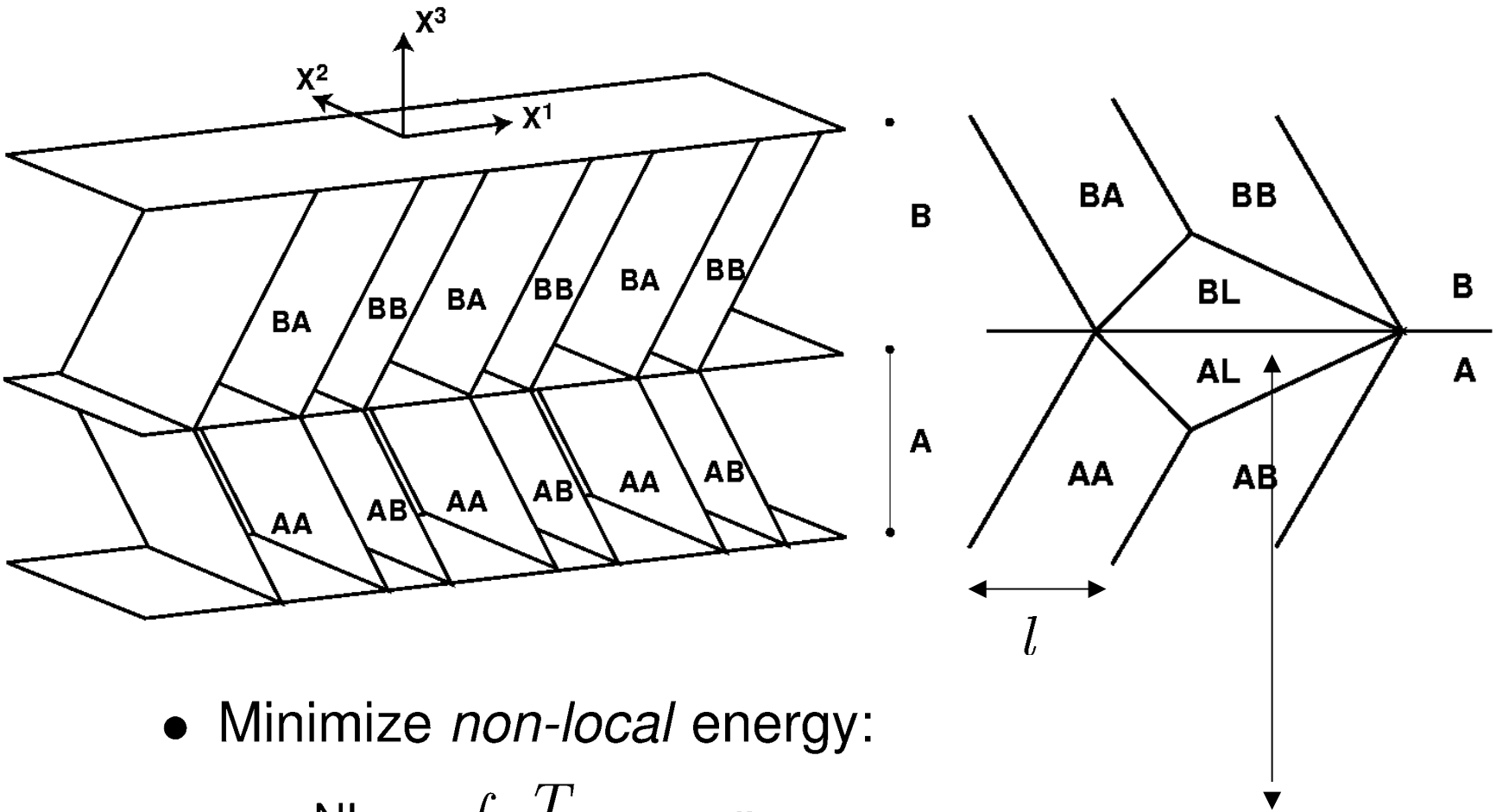

- Minimize *non-local* energy:

$$E^{\mathrm{NL}} \equiv \int_\Omega \frac{T}{b} |\mathrm{curl}\boldsymbol{F}^p_{n+1}|\, dx + \text{misfit energy}$$

Indentation of Cu-Al-Ni - Unrelaxed

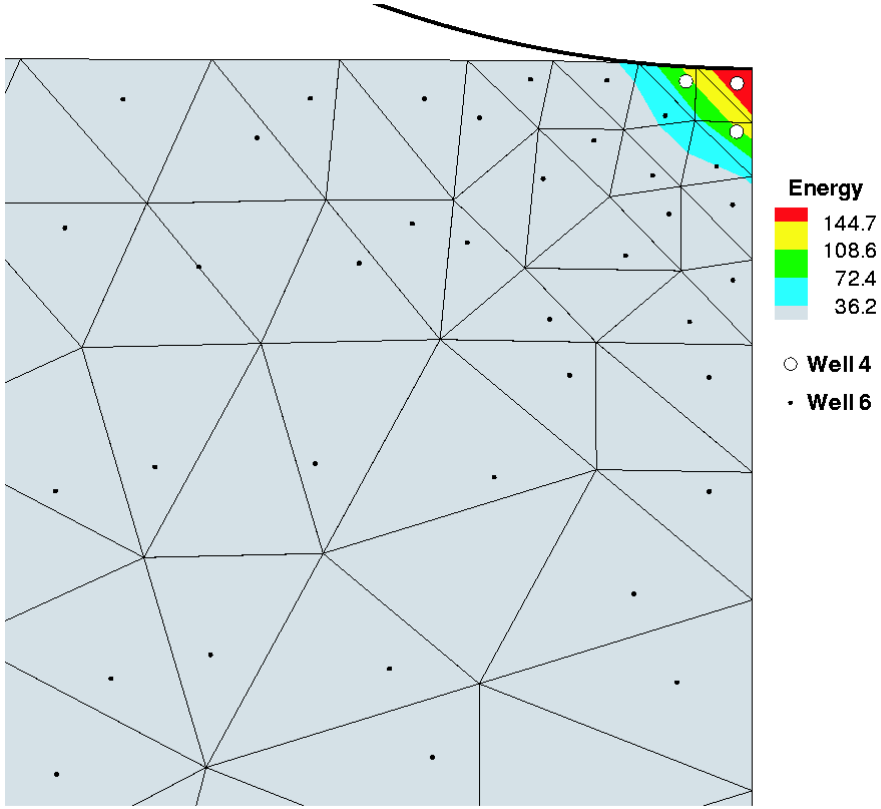

Indentation = 0.15

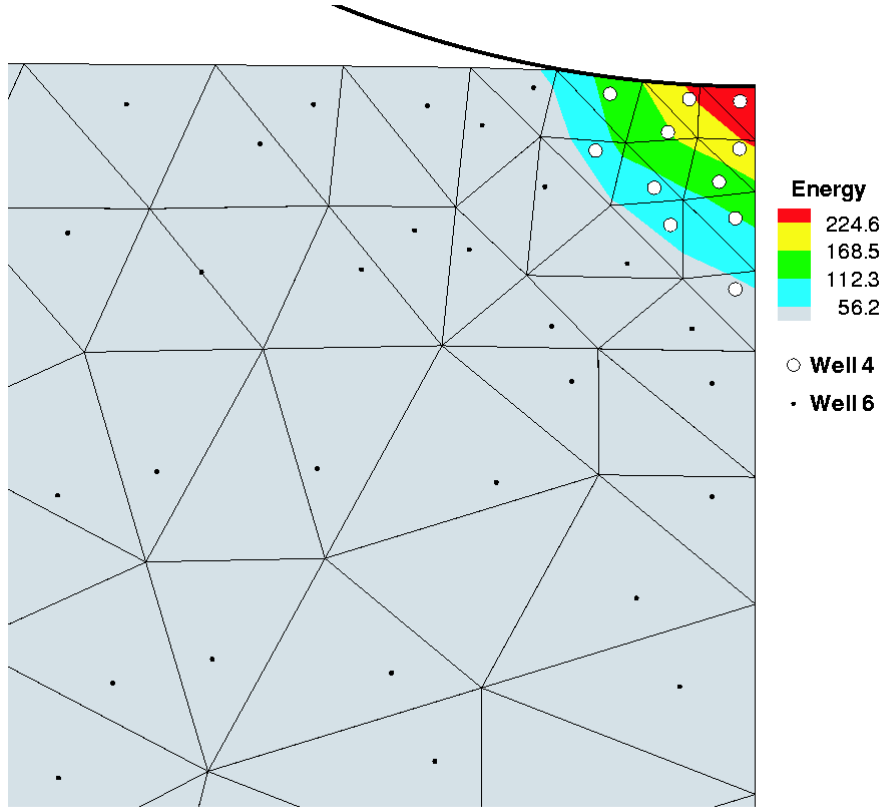

Indentation = 0.375

Michael Ortiz
GAMM 2002

Indentation of Cu-Al-Ni - Relaxed

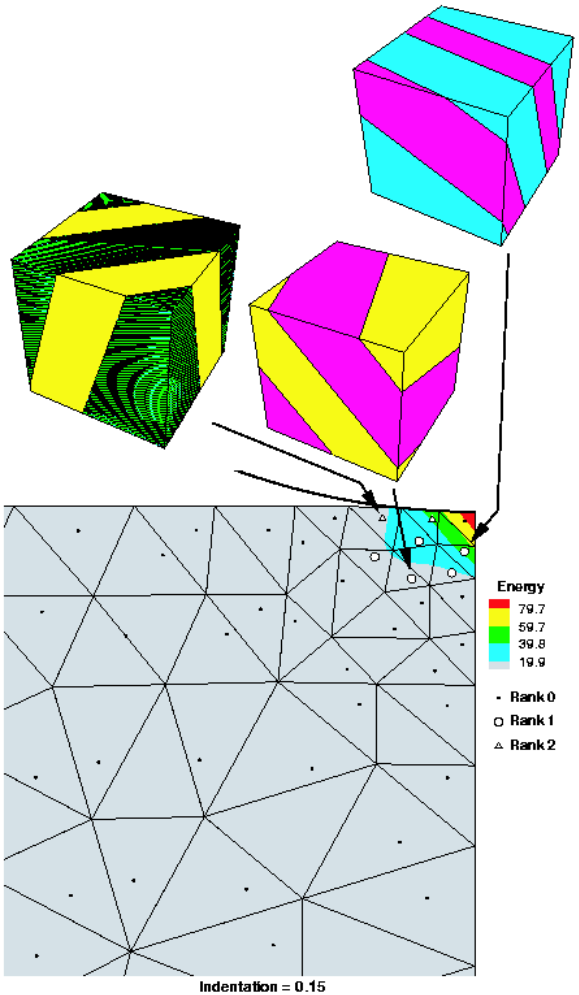

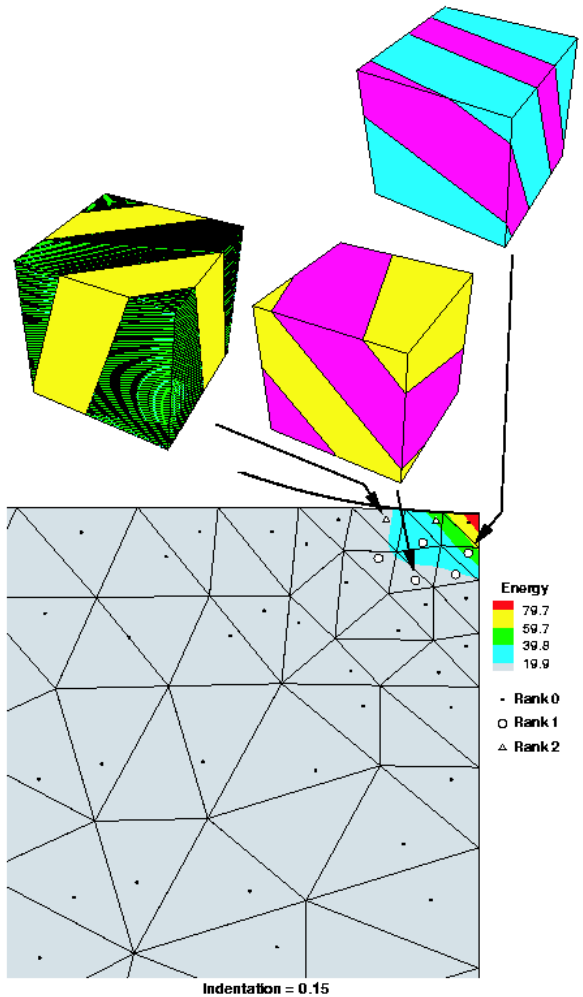

Michael Ortiz
GAMM 2002

Indentation of Cu-Al-Ni

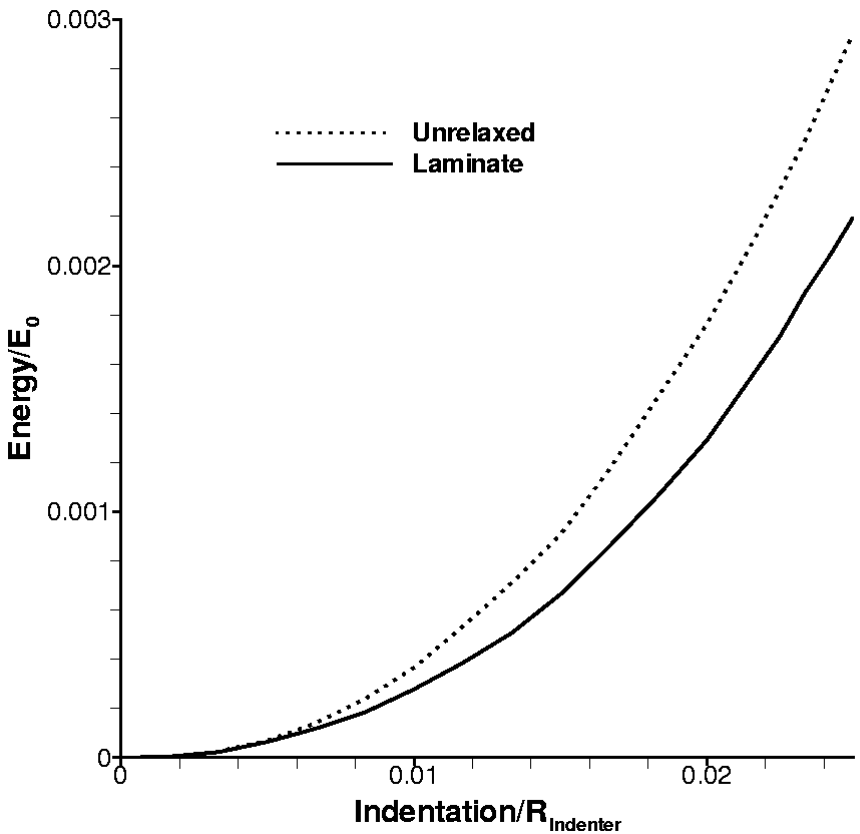

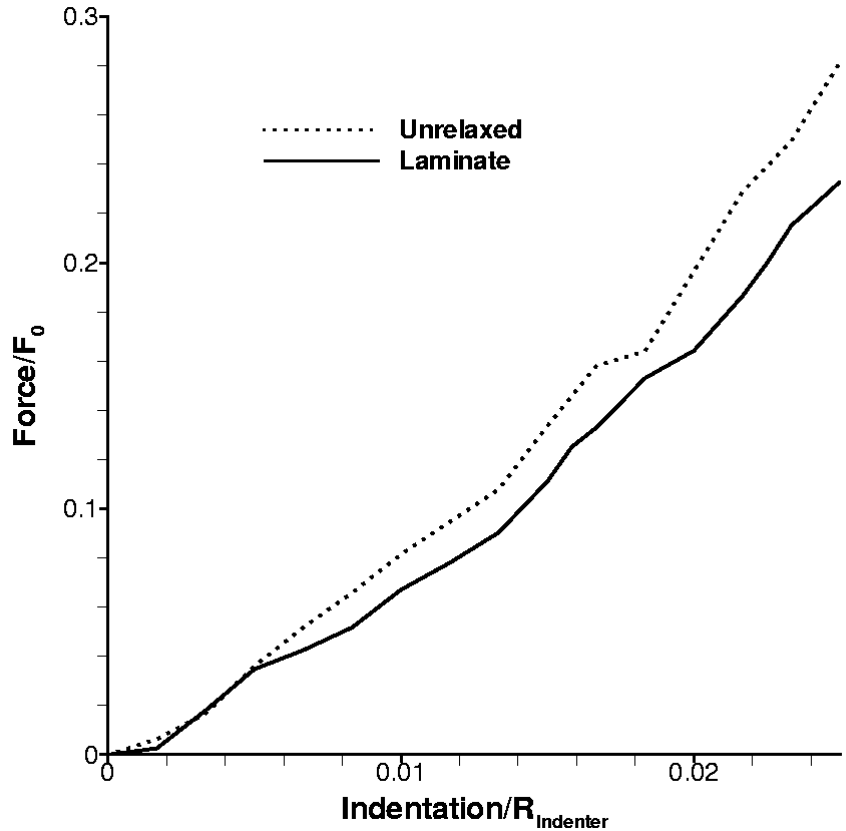

Michael Ortiz
GAMM 2002

Validation – Cold rolled polycrystalline Al

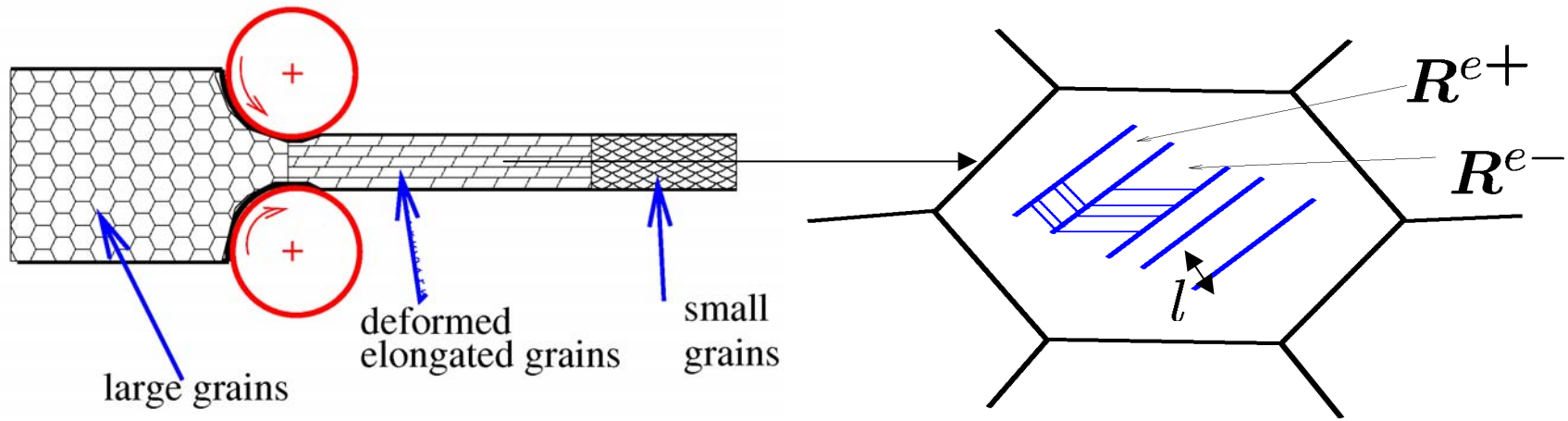

- Lattice rotation: $\boldsymbol{F} = \boldsymbol{F}^e\boldsymbol{F}^p,\ \ \boldsymbol{F}^e = \boldsymbol{R}^e\boldsymbol{U}^e$
- Relative rotation across walls: $\boldsymbol{R} = \boldsymbol{R}^{e+}(\boldsymbol{R}^{e-})^{-1}$
- *Misorientation angle*: $\theta = \text{angle}(\boldsymbol{R})$
- *Lamellar width*: l
- Calculations done for $\boldsymbol{F} = \text{diag}\{1/\lambda, \lambda, 1\}$, and 1000 random initial crystal orientations.

Validation – Cold rolled polycrystalline Al

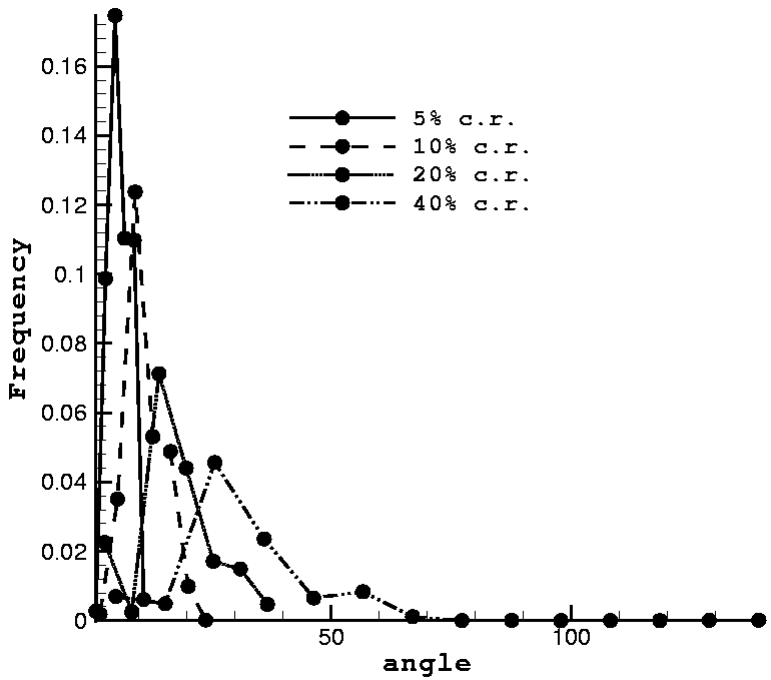

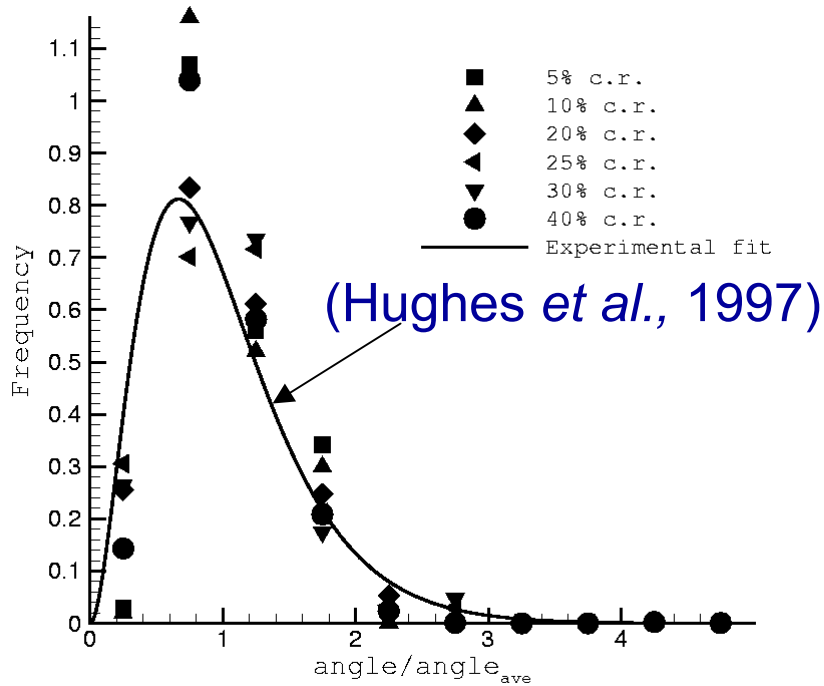

Misorientation-angle probability functions

Michael Ortiz
GAMM 2002

Validation – Cold rolled polycrystalline Al

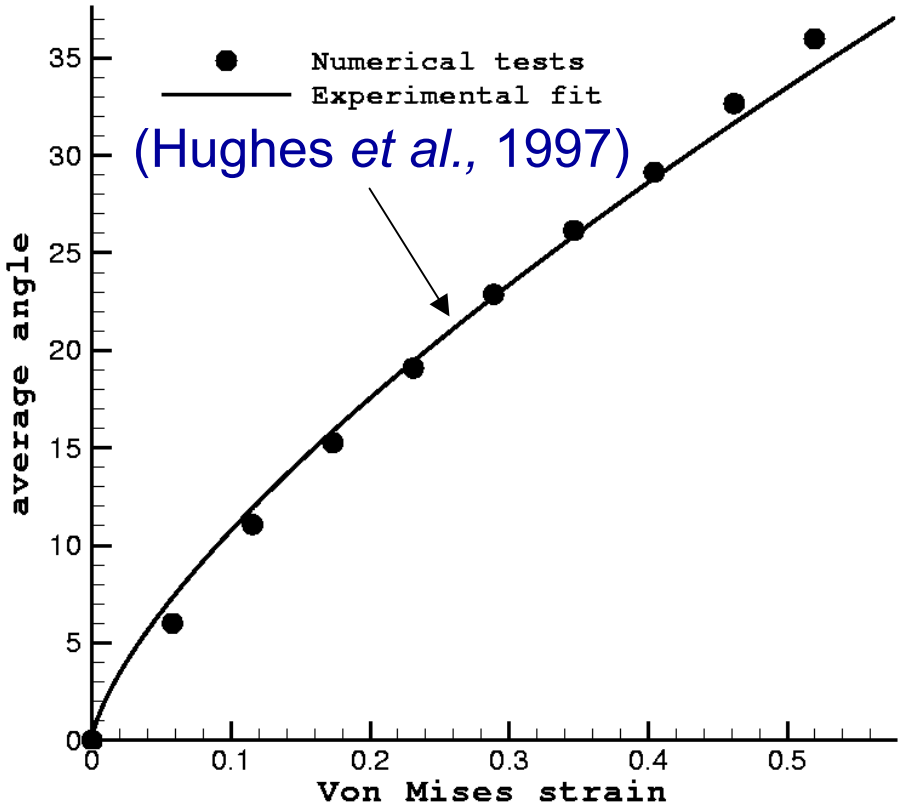

Average misorientation angle *vs* von Mises strain

Validation – Cold rolled polycrystalline Ni

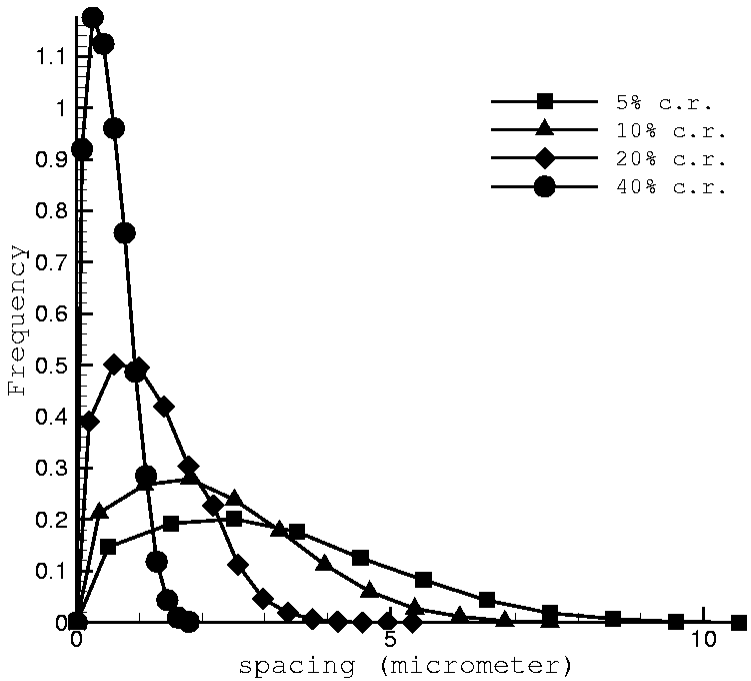

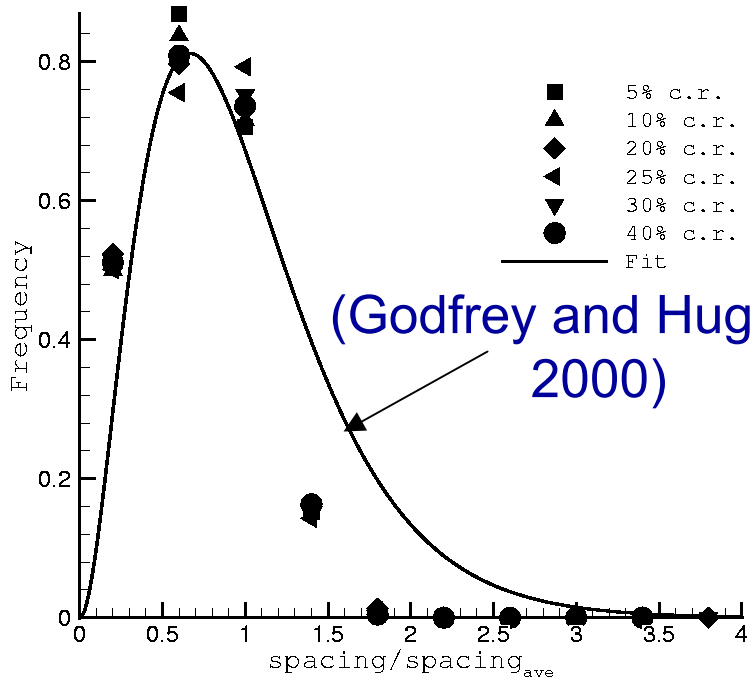

(Godfrey and Hughes, 2000)

Lamellar-width probability functions

Michael Ortiz
GAMM 2002

Validation – Cold rolled polycrystalline Ni

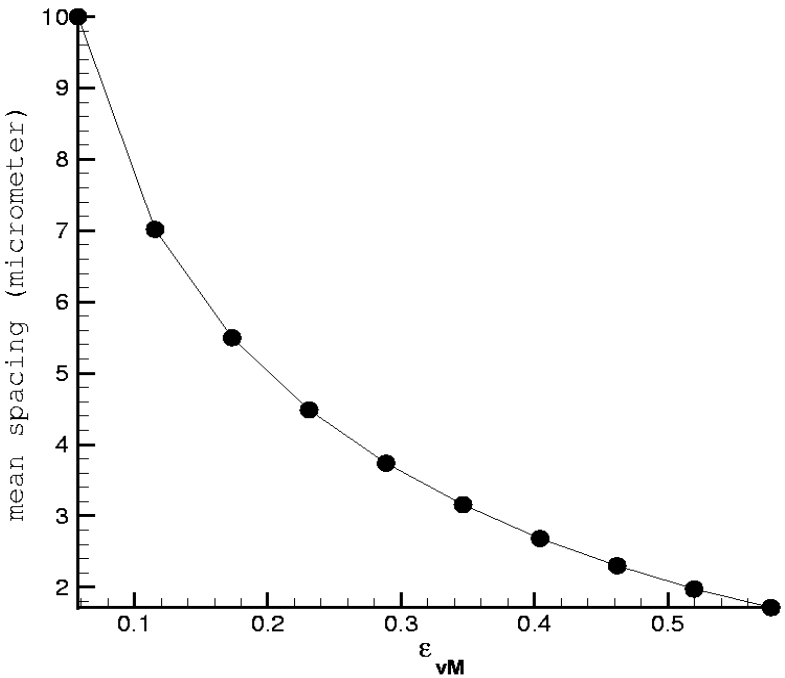

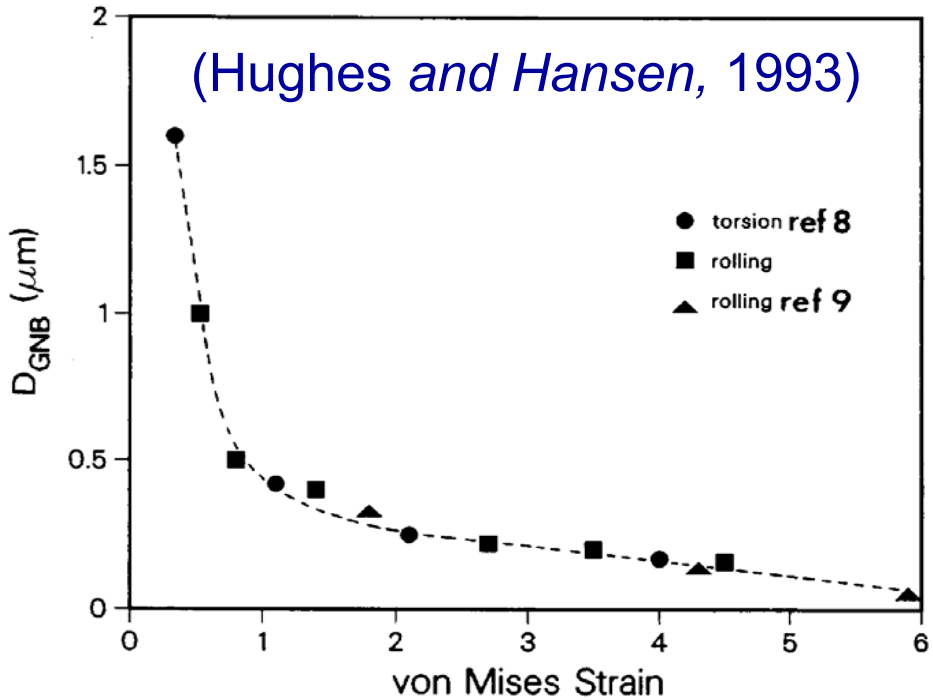

Mean spacing *vs* von Mises strain

Michael Ortiz
GAMM 2002

Summary and concluding remarks

- The incremental IBVP of finite-deformation single-crystal plasticity may be reduced to a sequence of minimization problems by recourse to variational constitutive updates
- For crystals with strong latent hardening the work-of-deformation functional is non-convex, which promotes fine microstructure
- Relaxation (probably) requires consideration of sequential laminates of finite depth only
- Multiscale approach:
  - *Finite elements endowed with effective behavior, no enhancement*
  - *Effective behavior computed by lamination algorithm at Gauss points*
- Theory predicts:
  - *Dipolar walls in fatigued fcc crystals (Ortiz and Repetto, JMPS, 1999)*
  - *Hall-:Petch scaling (Ortiz et al., JMPS, 2001).*
  - *Misorientation and spacing data (Aubry and Ortiz, Proc. Roy. Soc. London, submitted for publication).*